

AERO-THERMO-ELASTIC STABILITY ANALYSIS OF MULTI-LAYERED VISCO-ELASTIC PANELS

Enrico Zappino¹, Matteo Filippi¹, Erasmo Carrera¹

¹Mul² Team, Politecnico di Torino, Corso Duca degli Abruzzi, 24, 10129 Torino, Italy.

enrico.zappino@polito.it

matteo.filippi@polito.it

erasmo.carrera@polito.it

Keywords: Aero-elastic, Visco-elastic, Thermo-elastic, CUF

Abstract: In this paper the aero-thermo-elastic response of layered panels including the effects of viscoelastic materials is investigated. The structural models has been developed in the frameworks of the Carrera Unified Formulation that allows refined kinematics models to be derived without any *ad hoc* formulation. The aerodynamic forces have been evaluated by means of the piston theory that is only supersonic regimes have been considered. The aero-thermo-elastic model has been assessed and the effects of the viscoelastic material on the aeroelastic response have been evaluated. The results show that use of an advanced kinematics approximation leads to accurate results also when complex multi-layered panels are considered. The introduction of viscoelastic materials is able to modify the response of the panel and can be used to modify the range in which the aeroelastic instabilities appear.

INTRODUCTION

Panel flutter is an aeroelastic phenomenon that can cause failure of panels of wings, fuselages and missiles. It happens mostly at supersonic regime even though it can be observed in subsonic ranges. The panel flutter phenomena may appear in space structures during the coasting phase. Some non- destructive aeroelastic phenomena were detected on Saturn V rockets, and analytical and experimental test was carried out as shown by Nichols [1]. Moreover, the supersonic flight may lead to thermal loads due to the aerodynamic effects, these loads can afflict the aeroelastic instability and make it appear early. During the design of aerospace structures, especially in the case of thin-walled structure, the aeroelastic response have to be considered in order to avoid catastrophic events. In order to avoid the panel flutter phenomena an accurate design of the dynamic response of a structure is required. The possibility to modify the natural frequencies of a structure may move the flutter phenomena out from the critical mission regimes. In this sense, the use of innovative materials could lead to an improvements of the aeroelastic behavior of a structure. In this work, the effects on the aero-thermo-elastic instabilities of the use of viscoelastic materials in multi-layered panels have been investigated. The mechanical properties of the viscoelastic materials depend on the frequencies in which they are vibrating [2], the dynamic response of a panel could be, therefore, modified with the use of such materials. On the other and the analysis of these materials requires an iterative solution, see [3] that makes the solution time consuming, the use of efficient numerical models is therefore mandatory. The aero-thermo-elastic analysis of elastic and viscoelastic multi-layered panels is performed by using a refined one-dimensional theory based on the Carrera Unified Formulation, CUF [4–6]. The

aerodynamic model is based on the linear piston theory [7] therefore only supersonic regimes are considered. The results show that the use of refined structural models is able to provide accurate results in the description of the aeroelastic response of a multi-layered panel. The use of an advanced kinematics approximation, provided by the refined 1D models, through the panel thickness leads to accurate results also when complex multi-layered panels are considered. The introduction of viscoelastic materials is able to modify the response of the panel and can be used to modify the range in which the aeroelastic instabilities appear.

AERO-THERMO-ELASTIC MODEL

The aero-thermo-elastic model used in the present paper can be written in its general formulation using the Principle of Virtual Displacements, PVD:

$$\delta L_{int} + \delta L_{ine} + \delta L_{\sigma T} = \delta L_{ext} \quad (1)$$

where: L_{int} is the internal virtual work due to the elastic forces, L_{ine} is the work due to the inertial forces, and L_{ext} is the work due to the external forces; δ denotes virtual variations. If none of the external loads, except the aerodynamic forces, are considered, the terms δL_{ext} can be written as δL_a where L_a stands for the work of the aerodynamic loads.

$L_{\sigma T}$ is the work done by the initial stress distribution due to the thermal load. If the FEM is used to solve the problem, the virtual works can be written in matrix form. Equation 1 therefore becomes:

$$([K] + [K_a] + [K_{\sigma T}]) \{q\} + [D_a] \{\dot{q}\} + [M] \{\ddot{q}\} = 0 \quad (2)$$

where $[K]$ is the stiffness matrix, $[M]$ is the mass matrix, $[K_a]$ is the aerodynamic stiffness matrix and $[D_a]$ is the aerodynamic damping matrix. $[K_{\sigma T}]$ is the geometrical stiffness due to the thermal load. The structural damping and the flow inertia can be neglected. Each of these matrices is derived in explicit form in the following sections. The solution of Eq. 2 in the frequency domain leads to the solution of a Quadratic Eigenvalues Problem (QEP). Because of the introduction of viscoelastic effects the mechanical properties of materials must be considered frequency dependent, that is, the solution of the eigenvalues problem should be iterative. In order to avoid this time consuming approach the frequency responses solution is adopted where possible. The details of the solution approach are herein omitted for the sake of brevity, but can be found in the works by Carrera and Zappino [5] and Carrera and Filippi [8].

Advanced one-dimensional elements

The structural models used in the present work are derived using the CUF. The one-dimensional formulation is considered. More details about FE models derived via CUF can be found in the book by Carrera *et al.* [4]. In the framework of the CUF [4, 9], for a 1D problem, the displacement field \mathbf{u} is written as the product of two functions, a cross-sectional expanding function F_τ and the generalized displacement vector unknown \mathbf{u}_τ on the y-axis:

$$\mathbf{u}(x, y, z) = F_\tau(x, z) \mathbf{u}_\tau(y) \quad (3)$$

where index τ ranges from 1 to the number of terms of the expansion of order N .

When the Taylor, TE, 1D models are used, an expansion that uses 2D polynomials $x^m z^n$, as F_τ is considered, where m and n are positive integers. For instance, second-order displacement field reads:

$$\begin{aligned} u_x &= u_{x_1} + x u_{x_2} + z u_{x_3} + x^2 u_{x_4} + xz u_{x_5} + z^2 u_{x_6} \\ u_y &= u_{y_1} + x u_{y_2} + z u_{y_3} + x^2 u_{y_4} + xz u_{y_5} + z^2 u_{y_6} \\ u_z &= u_{z_1} + x u_{z_2} + z u_{z_3} + x^2 u_{z_4} + xz u_{z_5} + z^2 u_{z_6} \end{aligned} \quad (4)$$

Timoshenko theory (TBT) can be derived as a particular case by considering only the terms:

$$\begin{aligned} u_x &= u_{x_1} \\ u_y &= u_{y_1} + x u_{y_2} + z u_{y_3} \\ u_z &= u_{z_1} \end{aligned} \quad (5)$$

It can be shown that Euler-Bernoulli beam theory (EBBT) can be derived by introducing a penalization on the shear terms of the TBT model (see [10]).

In the case of LE models, Lagrange polynomials are used to build 1D higher-order theories. Two types of cross-section polynomial set are adopted in this paper: nine-point LE 9, and four-point LE 4. The isoparametric formulation is exploited to deal with arbitrary cross-section shaped geometries. For instance, LE 4 interpolation functions are:

$$\begin{aligned} F_1 &= \frac{1}{4}(1 - \xi)(1 - \eta) & F_2 &= \frac{1}{4}(1 + \xi)(1 - z) \\ F_3 &= \frac{1}{4}(1 + \xi)(1 + \eta) & F_4 &= \frac{1}{4}(1 - \xi)(1 + \eta) \end{aligned} \quad (6)$$

Where ξ and η are the coordinates in the natural reference system. Equation 6 coincides with the linear Lagrange polynomial in two dimensions. Using LE the unknowns are only the displacements of the cross-sectional nodes.

The FEM is used to approximate the displacement along the beam axis. In particular, the generalized displacement vector, $u_\tau(y)$, is linearly interpolated using the classical shape functions. When a beam element with N_{NE} nodes along the axis is considered, the generalized displacement vector becomes:

$$\mathbf{u}_\tau(y) = N_i(y)\mathbf{q}_{i\tau}; \quad i = 1 \dots N_{NE} \quad (7)$$

In Eq. 7 the index i ranges from 1 to the number of nodes per element N_{NE} . Therefore, the displacement field can be written as follows:

$$\mathbf{u}(x, y, z) = F_\tau(x, z)N_i(y)\mathbf{q}_{i\tau} \quad (8)$$

Where index i indicates the node of the element along the y -axis. Three- and four-node refined beam elements were used along the y -axis in the present work.

Stress and strain formulation

The strain vector can be written as:

$$\boldsymbol{\varepsilon} = (\varepsilon_{xx} \ \varepsilon_{yy} \ \varepsilon_{xy} \ \varepsilon_{xz} \ \varepsilon_{yz} \ \varepsilon_{zz})^T \quad (9)$$

It can be written in terms of displacements using the relation:

$$\boldsymbol{\varepsilon} = \mathbf{D}\mathbf{u} \quad (10)$$

The matrix \mathbf{D} contains the geometrical relations between the displacements and the strains. The explicit form of matrix \mathbf{D} can be found in the works by in the book by Carrera *et al.* [4]. The stress vector can be derived using the constitutive equations,

$$\boldsymbol{\sigma} = \mathbf{C}\boldsymbol{\varepsilon} \quad (11)$$

where \mathbf{C} is the matrix of the material coefficients and $\boldsymbol{\sigma}$ is the stress vector,

$$\boldsymbol{\sigma} = (\sigma_{xx} \ \sigma_{yy} \ \sigma_{xy} \ \sigma_{xz} \ \sigma_{yz} \ \sigma_{zz})^T \quad (12)$$

When Viscoelastic material are considered, the material coefficients can be function of the frequency of vibration. In this paper, the complex modulus approach has been used to define the viscoelastic materials properties. According to this methodology, the usual engineering moduli are defined as complex quantities. For example, the Youngs modulus is

$$E(i\omega) = E_{c0}(\omega)(1 + i\eta_c(\omega)) \quad (13)$$

where $E_{c0}(\omega)$ is the storage modulus, $\eta_c(\omega)$ is the corresponding material loss factor, and $i = \sqrt{-1}$.

Thermal stresses

The initial thermal stresses can be written as:

$$\sigma^\theta = \lambda\Delta T = \mathbf{C}\alpha\Delta T \quad (14)$$

Where ΔT is the temperature variation and α denotes the thermal expansion coefficients.

Elastic Work: Stiffness Matrix [K]

The internal work, δL_{int} , can be expressed in terms of elastic energy using the equations introduced in the section above.

$$\begin{aligned}\delta L_{int} &= \int_V (\delta \boldsymbol{\varepsilon}^T \boldsymbol{\sigma}) dV = \\ &= \delta \mathbf{q}_{\tau i}^{kT} \left[\int_V \mathbf{D}^T \left(N_i(y) F_\tau(x, z) \mathbf{I} \right) \mathbf{C}^k(\omega) \right. \\ &\quad \left. \left(N_j(y) F_s(x, z) \mathbf{I} \right) \mathbf{D} dV \right] \mathbf{q}_{s j}^k\end{aligned}\quad (15)$$

The variation of the internal work can be written, in terms of the fundamental nucleus of the stiffness matrix, as follows:

$$\delta L_{int} = \delta \mathbf{q}_{\tau i}^{kT} \mathbf{k}^{kij\tau s} \mathbf{q}_{s j}^k \quad (16)$$

where $\mathbf{k}^{kij\tau s}$ is the stiffness matrix in the form of the fundamental nucleus. The explicit forms of the 9 components of $\mathbf{k}^{kij\tau s}$ can be found in the book by Carrera *et al.* [4].

Initial thermal stress [K $^\theta$]

The effects of the initial thermal stress can be included in the analysis considering the work done by the variation of the virtual non-linear strain, ε_{nl} , given by the von Karman Formulation, with the thermal initial stress, σ^θ :

$$\begin{aligned}\delta L_{\sigma^\theta} &= \delta \mathbf{q}_{\tau i}^{kT} \int_V \left(F_{\tau, x} N_i \sigma_{0xx}^\theta \mathbf{I} F_{s, x} N_j + F_\tau N_{i, y} \sigma_{0xy}^\theta \mathbf{I} F_{s, x} N_j + F_{\tau, z} N_i \sigma_{0xz}^\theta \mathbf{I} F_{s, x} N_j \right. \\ &\quad + F_{\tau, x} N_i \sigma_{0xy}^\theta \mathbf{I} F_{s, y} N_j + F_\tau N_{i, y} \sigma_{0yy}^\theta \mathbf{I} F_{s, y} N_j + F_{\tau, z} N_i \sigma_{0yz}^\theta \mathbf{I} F_{s, y} N_j \\ &\quad \left. + F_{\tau, x} N_i \sigma_{0xz}^\theta \mathbf{I} F_{s, z} N_j + F_\tau N_{i, y} \sigma_{0yz}^\theta \mathbf{I} F_{s, z} N_j + F_{\tau, z} N_i \sigma_{0zz}^\theta \mathbf{I} F_{s, z} N_j \right) dV \mathbf{q}_{s j}^k\end{aligned}\quad (17)$$

The variation of the work done by the initial stress field can be written, in terms of the fundamental nucleus, as follows:

$$\delta L_{\sigma^\theta} = \delta \mathbf{q}_{\tau i}^{kT} \mathbf{k}_\sigma^{\theta k i j \tau s} \mathbf{q}_{s j}^k \quad (18)$$

Where $\mathbf{k}_\sigma^{\theta k i j \tau s}$ is the fundamental nucleus of the stiffness matrix due to the initial thermal stress.

Inertial Work: Mass Matrix [M]

The mass matrix formulation is derived from the variation of the work made by the inertial forces:

$$\delta L_{ine} = \int_V \delta \mathbf{u}^k \cdot \ddot{\mathbf{u}}^k \cdot \rho^k(z) dV \quad (19)$$

where the dot denotes derivatives with respect to time and the double dot denotes acceleration. After substitution of eq.8 in eq.19, one obtains:

$$\begin{aligned}\delta L_{ine} &= \delta \mathbf{q}_{i\tau}^{kT} \left[\int_V \left(F_\tau(z) \mathbf{I} N_i(y) \rho^k \right. \right. \\ &\quad \left. \left. N_j(y) F_s(x, z) \mathbf{I} \right) dV \right] \ddot{\mathbf{q}}_{s j}^k = \\ &= \delta \mathbf{q}_{i\tau}^{kT} \mathbf{m}^{k i j \tau s} \ddot{\mathbf{q}}_{s j}^k\end{aligned}\quad (20)$$

where $\mathbf{m}^{kij\tau s}$ is the mass matrix, which is a function of the shape functions N_i , F_τ and of the material density ρ^k on the k - th layer.

Aerodynamic model

The aerodynamic model used in the present work is based on the Piston Theory. This model was first used in aeroelastic analysis by Ashley and Zartarian [7]; it has an easy formulation and it provides accurate results in the supersonic range, for Mach numbers greater than 1.7. The piston theory assumes that the flow on a panel is similar at a one-dimensional flow in a channel (e.g. in a piston). The flow velocity is assumed to be parallel to the surface and the vertical velocity \dot{u}_z can therefore be expressed in two dimensional form as:

$$\dot{u}_z = \frac{\partial u_z}{\partial t} \pm V_\infty \frac{\partial u_z}{\partial y} \quad (21)$$

There are two contributions: the former is due to the vertical displacement, and the latter is due to the surface slope. The sign of velocity V_∞ depends on its direction: it is positive if V_∞ is in the positive yx - *direction* and negative if V_∞ is in the negative y - *direction*. The differential pressure across a panel can therefore be expressed as:

$$\Delta p(y, t) = \frac{2q}{M} \left\{ \frac{\partial u_z}{\partial y} + \frac{1}{V_\infty} \frac{\partial u_z}{\partial t} \right\}. \quad (22)$$

Eq.22 shows that the local differential pressure is a function of the velocity of the normal displacement and of the slope of the surface. A refined formulation has been proposed by Krumhaar [11] for low supersonic ranges:

$$\Delta p(y, t) = \frac{2q}{\sqrt{M^2 - 1}} \left\{ \frac{\partial u_z}{\partial y} + \frac{M^2 - 2}{M^2 - 1} \frac{1}{V_\infty} \frac{\partial u_z}{\partial t} \right\} \quad (23)$$

It is easy to see that when the Mach number goes to infinity, the eq.23 coincides with eq.22. In this work, eq.23 is used to compute the virtual work related to the aerodynamic forces. The differential pressure, acting on the panel, given by eq.23, can be expressed as the sum of two terms:

$$\Delta p(y, t) = \pm A \frac{\partial u_z}{\partial y} + B \frac{\partial u_z}{\partial t} \quad (24)$$

where:

$$A = \pm \frac{2q}{\sqrt{M^2 - 1}}; \quad B = \frac{2q}{\sqrt{M^2 - 1}} \frac{M^2 - 2}{M^2 - 1} \frac{1}{V_\infty}. \quad (25)$$

The first term, $(\pm A \frac{\partial u_z}{\partial y})$, represents a contribution to the stiffness of the problem, and it is therefore called *aerodynamic stiffness*. The second term, $(B \frac{\partial u_z}{\partial t})$, depends on the vertical velocity and it may be interpreted as a damping; it is therefore called *aerodynamic damping*.

Aerodynamic Stiffness Matrix [K_a]

The aerodynamic stiffness matrix may be derived by evaluating the work, δL_{aer} , made by a differential pressure, Δp , due to the slope of the surface in the flow direction.

$$\delta L_{aer}^A = \int_{\Lambda} (\delta \mathbf{u}^k \Delta p^A) d\Lambda \quad (26)$$

where index A indicates that only the contribution of the slope is considered, and Λ is the surface where the pressure acts. Considering the formulation proposed in eq.24, and introducing the displacement formulation reported in eq.8, differential pressure can be written as:

$$\Delta p^A = A \frac{\partial u_z}{\partial y} = A \cdot I_{\Delta p} \frac{\partial N_i}{\partial y} F_{\tau} q_{i\tau}^k \quad (27)$$

where:

$$I_{\Delta p} = \begin{bmatrix} 0 & 0 & 0 \\ 0 & 0 & 0 \\ 0 & 0 & 1 \end{bmatrix} \quad (28)$$

Since $d\Lambda = dx \cdot dy$, and substituting eq.27 in eq.26, the virtual work of the differential pressure can be written as:

$$\delta L_{aer}^A = \delta q_{js}^{kT} \left[A \left(\int_x F_{\tau} F_s dx \right) \int_L N_j \frac{\partial N_i}{\partial y} I_{\Delta p} dy \right] q_{i\tau}^k = \delta q_{js}^{kT} \mathbf{k}_a^{kij\tau s} q_{i\tau}^k \quad (29)$$

where $\mathbf{k}_a^{kij\tau s}$ is the aerodynamic stiffness matrix which may be written in the form:

$$\mathbf{k}_a^{kij\tau s} = \frac{2q}{\sqrt{M^2 - 1}} \int_x F_{\tau} F_s dx \begin{bmatrix} 0 & 0 & 0 \\ 0 & 0 & 0 \\ 0 & 0 & \int_L N_j \frac{\partial N_i}{\partial y} dy \end{bmatrix} \quad (30)$$

Aerodynamic Damping Matrix [D_a]

The aerodynamic damping matrix may be derived by evaluating the work, δL_{aer} , made by a differential pressure, Δp , due to the vertical displacement velocity of the surface.

$$\delta L_{aer}^B = \int_{\Lambda} (\delta \mathbf{u}^k \Delta p^B) d\Lambda \quad (31)$$

where index B indicates that only the contribution of the vertical displacement velocity is considered. Considering the formulation proposed in eq.24 and introducing the displacement formulation reported in eq.8, differential pressure can be written as:

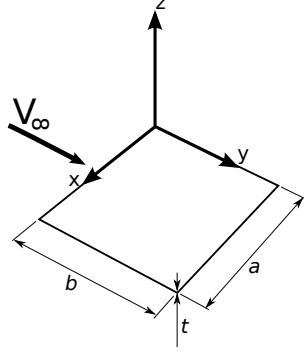


Figure 1: Panel geometrical configuration and System of reference

$$\Delta p^B = B \frac{\partial u_z^k}{\partial t} = B \cdot F_\tau N_i I_{\Delta p} \frac{\partial q_{i\tau}^k}{\partial t} \quad (32)$$

$$\delta L_{aer}^B = \delta q_{js}^{kT} \left[B \left(\int_x F_\tau F_s dx \right) \int_L N_i N_j I_{\Delta p} dy \right] \frac{\partial q_{i\tau}^k}{\partial t} = \delta q_{js}^{kT} \mathbf{d}_a^{kij\tau s} \frac{\partial q_{i\tau}^k}{\partial t} \quad (33)$$

where $\mathbf{D}_a^{jj\tau s}$ is the aerodynamic damping matrix which may be written in the following form:

$$\mathbf{d}_a^{kij\tau s} = \frac{2q}{\sqrt{M^2 - 1}} \frac{1}{V_\infty} \left(\frac{M^2 - 2}{M^2 - 1} \right) \int_x (F_\tau F_s) dx \begin{bmatrix} 0 & 0 & 0 \\ 0 & 0 & 0 \\ 0 & 0 & \int_\Lambda N_i N_j dx dy \end{bmatrix} \quad (34)$$

NUMERICAL RESULTS

This section shows some results obtained using the aero-visco-elastic model introduced in the sections above. Two main problems are considered. The first concerns the aeroelastic response of a thin panel. The aero-elastic has been assessed in order to prove the accuracy of the proposed approach. The second problem considers the aero-visco-elastic response of a multi-layered panel.

Aero-elastic response of an isotropic panel

In order to assess the present aeroelastic model, a simply supported panel has been investigated and the results have been compared with those from literature [12]. The panel has the geometry reported in fig.1. The length, b , is considered equal to 0.5 [m], the width, a , is equal to 1 [m] and the thickness, t , is equal to 0.002 [m]. The trailing edge and the leading edge are simply supported, while the side edges are free. The model is made of 12 beam elements. Two different displacement formulations have been used to describe the displacement on the cross section, a third order Taylor expansion (TE3) and a Lagrange formulation using 2 Q9 elements. The analyses were carried out considering a flow with a temperature, T , equal to 228 [K] and a density of 0.3639 [Kg/m³]. Fig.2 shows the frequencies and the damping at different Mach numbers, between 1.5 and 8. It is possible to see that there are three points of instability: P-1, P-2 and P-3. The values of the critical Mach numbers and frequencies of each point are

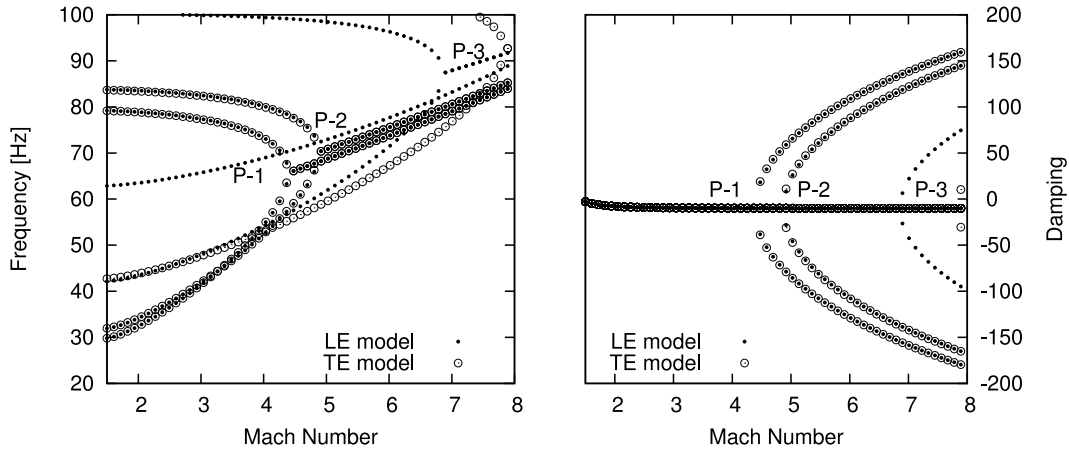
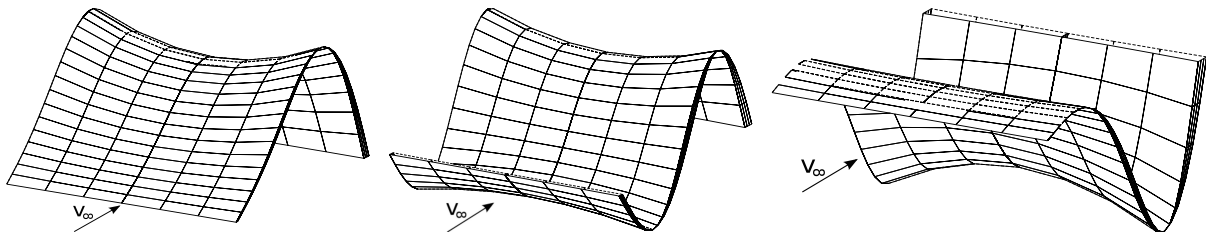


Figure 2: Simply supported panel, frequencies and damping at different Mach number, advanced TE and LE theory

Instability Point	EBBM		TE3		LE		Ref. [12]	
	Mach	Freq.[Hz]	Mach	Freq.[Hz]	Mach	Freq.[Hz]	Mach	Freq.[Hz]
P-1	4.03	60.04	4.47	66.08	4.47	66.09	4.5	66.00
P-2	-	-	4.92	70.35	4.91	70.37	-	-
P-3	-	-	7.89	92.68	6.89	87.48	-	-

Table 1: Critical Mach number and flutter Frequencies for a simply supported panel, comparisons with literature results

reported in tab.1, while the literature results are reported in the last column. In fig.s3, the modes involved in the first aeroelastic instability and the flutter mode are reported. Because of the quasi-3D solution achieved using the present model, the results can be given through a full 3D visualization. The results are very close to the results found in literature. The present higher-order models give a critical Mach number of 4.47 versus the 4.5 found in literature and the frequency is also similar, with 66.09 [Hz] for the present model and 66 [Hz] from literature. Different Flutter modes could appear: P-1 instability (fig.3) involves two bending modes. The classical structural model, EBBM, and the one used by [12] are not able to detect all the flutter modes, since they are not able to predict the torsional and shell-like modes. The TE3 model is able to predict this instability, but does not provide good accuracy because the third-order model does not offer a proper description of the involved modes; a higher order model needs to be used to obtain a better solution. The present assessment highlights that the TE and LE models are suitable for aeroelastic application and provide results that are in agreement with those from literature. Moreover, higher-order models can detect torsional and shell-like flutter instabilities.



(a) Mode 1, Mach number 1.5, 29.79 [Hz] (b) Mode 5, Mach number 1.5, 79.21 [Hz] (c) Instability P-1, Mach number 4.47, 66.09 [Hz]

Figure 3: Simply supported panel, modes involved in the aeroelastic instabilities P-1

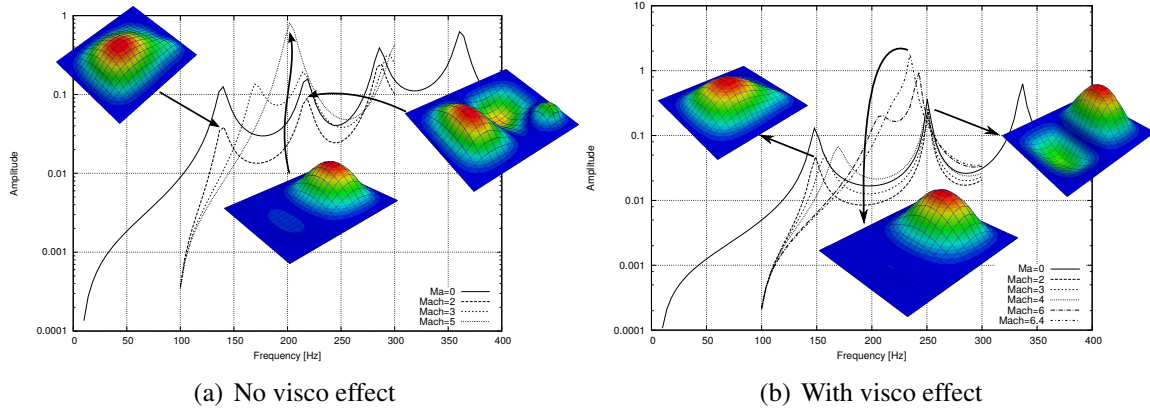


Figure 4: Frequency response and aeroelastic modes of the panel with and without the visco-elastic effect

Aero-visco-elastic response of an isotropic panel

The aero-visco-elastic response of a layered panel has been investigated in the present section. The panel has the geometry reported in fig.1. The length, b , is considered equal to 0.33 [m], the width, a , is equal to 0.39 [m]. A three layers layup has been considered. From the bottom the layers have a thickness of, 0.0015 [m], 0.0000254 [m] and 0.0004 [m] respectively. The outer layers have been built in aluminum while the middle layer is a viscoelastic layer (material *M3ISD112TM*). The model is fully clamped. Figure 4 show the aero-visco-elastic frequency response of the panel at different Mach numbers including the modal shapes involved in the instability. Table 2 show the critical Mach numbers and the critical frequencies for the plate

Model	Critical Mach	Freq.[Hz]
Multilayered panel (without visco effects)	~ 5.0	~ 204
Multilayered panel (with visco effect)	$\sim 6.4(+28\%)$	$\sim 235(+15\%)$

Table 2: Critical velocities of the viscoelastic panel with and without the viscoelastic effect.

with and without the viscoelastic effect. When the viscoelastic effect is not considered the properties of the material have been considered constant and equal to the properties at zero frequency. The results show that the introduction of the viscoelastic material may change the critical flutter condition, in this case the critical Mach number has been increased of the 28% while the critical frequency of the 15%.

CONCLUSION

An advanced structural model able to deal with the aero-elastic and aero-visco-elastic problem has been developed in this work. The formulation has been developed in the framework of the Carrera Unified Formulaiton that allows the matrices to be written in compact form. Different structural models, Equivalent Single Layer and Layer-Wise, have been considered. From the results it is possible to state that:

- The present model is able to provide accurate results for the aeroelastic response of thin panel;
- The use of refined model permits to obtain quasi-3D solution;
- Multi-layered panel including viscoelastic material can be easily investigated using a layer-wise approach;
- The use of the visco-elastic materials may be used to control the flutter phenomena.

In conclusion the present model appears to be very promising in the analysis of viscoelastic materials and it could be used to evaluate their effects on the aeroelastic instabilities.

REFERENCES

- [1] Nichols, J. (1969). Final report: Saturn v, s-ivb panel flutter qualification test. *NASA-TN-D-5439*.
- [2] Rao, M. D. (2003). Recent applications of viscoelastic damping for noise control in automobiles and commercial airplanes. *Journal of Sound and Vibration*, 262(3), 457 – 474. ISSN 0022-460X. doi:[http://dx.doi.org/10.1016/S0022-460X\(03\)00106-8](http://dx.doi.org/10.1016/S0022-460X(03)00106-8). 2001 India-USA Symposium on Emerging Trends in Vibration and Noise Engineering.
- [3] Ferreira, A., Araujo, A., Neves, A., et al. (2013). A finite element model using a unified formulation for the analysis of viscoelastic sandwich laminates. *Composites Part B: Engineering*, 45(1), 1258 – 1264. ISSN 1359-8368. doi:<http://dx.doi.org/10.1016/j.compositesb.2012.05.012>.
- [4] Carrera, E., Cinefra, M., M. Petrolo, and Zappino, E. (2014). *Finite Element Analysis of Structures Through Unified Formulation*. John Wiley & Sons. In press.
- [5] Carrera, E. and Zappino, E. (2014). Aeroelastic analysis of pinched panel in variable supersonic flow changing with altitude. *Journal of Spacecraft and Rockets*, 51(1), 187–199. doi:10.2514/1.A32363.
- [6] Carrera, E., Filippi, M., and Zappino, E. (2016). Aeroelastic instabilities analysis of elastic and viscoelastic multi-layered panels. In *Proceedings 14th European Conference on Spacecraft Structures, Materials and Environmental Testing*. doi:10.2514/6.2013-1701.
- [7] Ashley, H. and Zartarian, G. (1956). Piston theory - a new aerodynamic tool for the aeroelastician. *Composites Structures*, 1109–1118.
- [8] Filippi, M., Carrera, E., and Regalli, A. M. (2016). Layerwise Analyses of Compact and Thin-Walled Beams Made of Viscoelastic Materials. *Journal of Vibration and Acoustics*, 138(6), 64501. ISSN 1048-9002.
- [9] Carrera, E. and Giunta, G. (2010). Refined beam theories based on a unified formulation. *International Journal of Applied Mechanics*, 2(1), 117–143.
- [10] Carrera, E., Giunta, G., and Petrolo, M. (2011). *Beam Structures: Classical and Advanced Theories*. John Wiley & Sons Ltd. ISBN 9780470972007.
- [11] Krumhaar, H. (1963). The accuracy of linear piston theory when applied to cylindrical shells. *AIAA Journal*, 1, 1448–1449.
- [12] Krause, H. (1998). Flattern flacher schalen bei uberschallanstr omung.

COPYRIGHT STATEMENT

The authors confirm that they, and/or their company or organization, hold copyright on all of the original material included in this paper. The authors also confirm that they have obtained permission, from the copyright holder of any third party material included in this paper, to publish it as part of their paper. The authors confirm that they give permission, or have obtained permission from the copyright holder of this paper, for the publication and distribution of this paper as part of the IFASD-2017 proceedings or as individual off-prints from the proceedings.